

# Electron Spin Resonance, Confocal, Micro-Raman, and Emission Characterization of Femtosecond Laser Modified Regions in Poly (Methyl Methacrylate) and Poly (Dimethyl Siloxane)

K. L. N. Deepak<sup>1</sup>, D. Narayana Rao<sup>1</sup> and S. Venugopal Rao<sup>2</sup>

<sup>1</sup> School of Physics, University of Hyderabad, Hyderabad-500046, India

<sup>2</sup> Advanced Centre of Research in High Energy Materials,

University of Hyderabad, Hyderabad-500046, India

Email: dnrsp@uohyd.ernet.in, svrsp@uohyd.ernet.in

## Abstract

We have fabricated and characterized microstructures, micro-craters, and diffraction gratings (surface and buried) using femtosecond (fs) direct writing technique at different focal conditions, laser parameters, and scanning speeds. Herein, we present some of our results on Electron Spin Resonance (ESR), micro-Raman spectroscopy and emission characterization from the fs modified regions of Poly (Methyl Methacrylate) [PMMA] and Poly (Dimethyl Siloxane) [PDMS].

## Introduction

The fs laser has become a promising tool for micromachining primarily due to its superior benefits over continuous wave and long pulse lasers [1–3]. With long pulse lasers, substantial heat diffusion occurs during the laser–material interaction, resulting in relatively large volume of heat affected zone (HAZ) around the laser focus. However, in the case of short pulse interaction the pulse duration ( $\sim 100$  fs) is much shorter than the electron–ion energy transfer time [4]. During the laser pulse duration, the target material at focus is driven to much higher temperature and evaporated before the heat can diffuse away. Owing to lack of heat diffusion, the heating of the surrounding area is significantly reduced. Therefore, micromachining/writing with fs pulses is always accompanied with negligible HAZ, absence of liquid phase, and precise threshold [1, 4]. Another unique characteristic of a fs pulse is that it produces extremely high peak power. Several optical structures such as gratings, waveguides, couplers etc. can be fabricated in a single substrate using this technique [5–7].

## Experimental

Figure 1 shows schematic of the experimental set up. We used a Ti: sapphire amplifier operating at 800 nm

delivering 1 kHz,  $\sim 100$  fs pulses with a maximum energy of  $\sim 1$  mJ. The time-bandwidth product confirmed that pulses were near-transform limited. We utilized 40X (NA 0.65) and 20X (0.4 NA) objectives for focusing the ultrashort pulses. Three stages, capable of 17-nm resolution, were utilized to translate the sample in X, Y, and Z directions. High-quality PMMA (PDMS) samples of 1 mm (6 mm) thickness cut into 1 cm  $\times$  2 cm were typically used for writing the buried structures. Energy of the input laser was varied using half wave plate and polarizer. The writing was performed in the transverse geometry. A Supercontinuum spot was observed when the focused light coincided with polymer surface and the substrate was adjusted accordingly such that the light is either focused on the surface or well inside the surface. The energy values presented here are estimated at the sample accounting for all the losses in the experimental set up.

## Results and discussion

Initially, we fabricated diffraction gratings (surface and buried) using different focusing conditions for both PMMA and PDMS. We obtained the best first-order diffraction efficiency of 35% in case of buried gratings in PMMA (50  $\mu$ J, 250  $\mu$ m/s & 15  $\mu$ m period) and 10% in case of PDMS (3  $\mu$ J, 1 mm/s & 15  $\mu$ m period). To understand the physical changes that occurred due to fs pulses, we collected Raman, ESR, and emission spectra from the modified regions. Figure 2b shows the Raman spectrum of fs modified region using high energy (50  $\mu$ J, 250  $\mu$ m/s) while figure 3b shows spectra from modified region using low energy (3  $\mu$ J, 500  $\mu$ m/sec) achieved using a 40X objective. Figure 4b represents the Raman spectra obtained from a typical buried grating fabricated in PDMS (3  $\mu$ J, 500  $\mu$ m/s). All these three figures illustrate the Raman spectrum of pristine sample also for comparison.



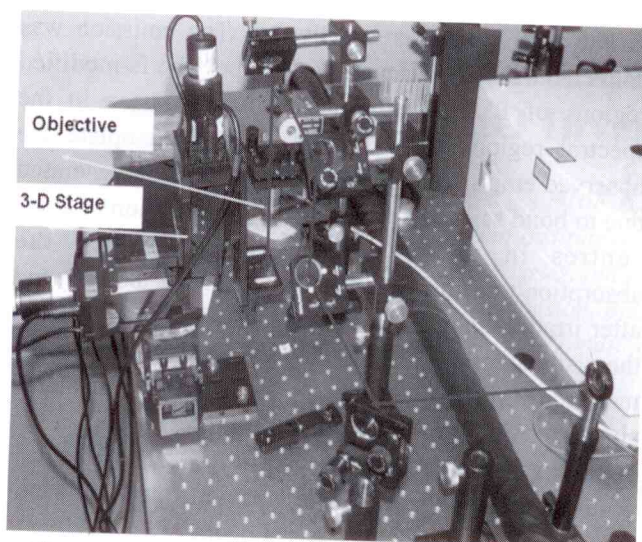


Figure 1 Experimental set up used for laser direct writing

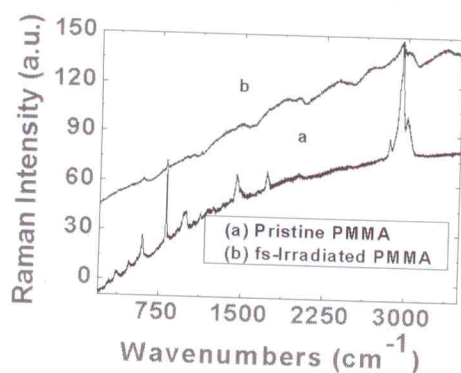


Figure 2 Raman spectrum of PMMA grating fabricated (50  $\mu$ J, 0.25 mm/sec, 15  $\mu$ m period) using 40X objective.

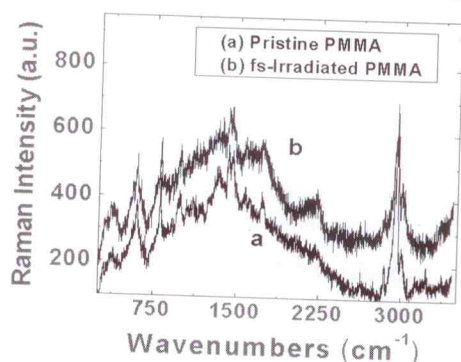


Figure 3 Raman spectrum of PMMA grating fabricated (3  $\mu$ J, 500  $\mu$ m/sec) with 40X objective.

Raman spectra from the fs modified regions indicated bond scission, softening, and stress related mechanisms responsible for structural changes. It is evident from figure 2 that various peaks were broadened drastically, probably due to huge strain created by the enormous peak intensities, and thereby the shockwaves created, at focal volume. It is possible that broadening could result from the pressure-driven structural

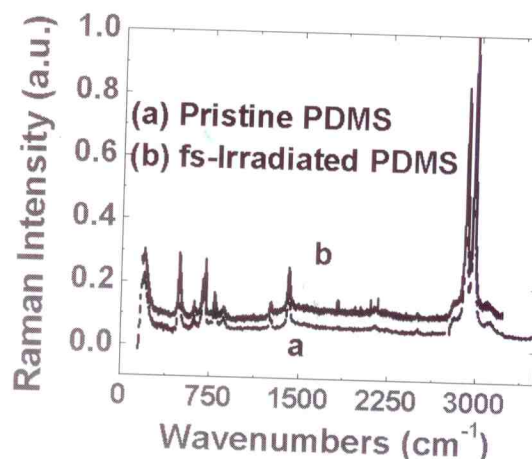


Figure 4 Raman spectrum of PDMS grating (3  $\mu$ J energy, 500  $\mu$ m/s, 10  $\mu$ m period) using 40X objective.

disordering at high energies. Grating fabricated (figure 3) with  $\sim 3$   $\mu$ J energy has shown less broadened peaks compared to that of grating fabricated at high energy (figure 2). We believe that additional pressure driven structural disordering had occurred in the later case. Raman spectrum of fs modified PDMS (figure 4) demonstrated that there was no alteration in position/peak width in different regions. A slight change in Raman intensity of the modified regions compared to unmodified regions was noticed, which could be due to scattering. We had collected the ESR signal to check the formation of free radicals due to bond breakage after fs laser irradiation. Figures 5 and 6 illustrate the ESR spectra of modified PMMA and PDMS, respectively. We did not observe any ESR signal from the regions of modified PMMA since the spectrum was collected 5 days after exposure. However, samples of PMMA that are mechanically scratched and recorded immediately showed ESR signal. In case of PDMS, even after 5 days we could see the ESR signal. Both mechanically modified PMMA and femtosecond irradiated PDMS

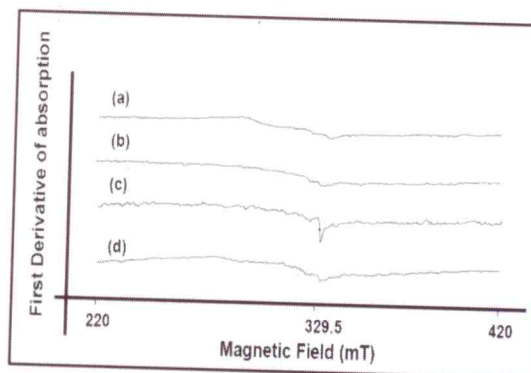
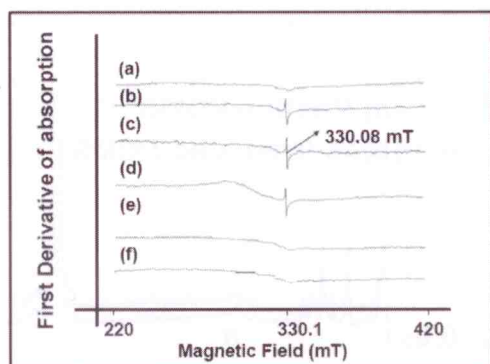
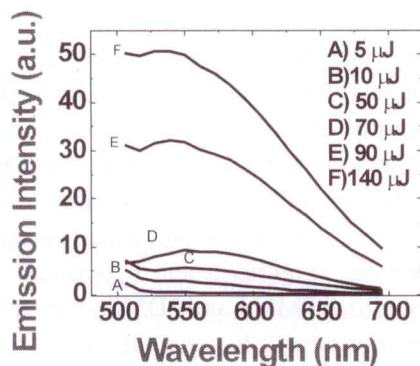


Figure 5 (a) Pristine PMMA (b) fs irradiated PMMA (c) mechanically scratched PMMA (d) mechanically scratched PMMA after 90 minutes



**Figure 6** (a) Pristine PDMS  
(b)-(e) fs irradiated PDMS at 3, 6, 30  $\mu\text{J}$  energies  
(e) mechanically scratched PDMS  
(f) mechanically scratched PDMS after 15 minutes

have shown ESR signal at 330 mT. Hence, we feel that the same free radical (probably peroxide radical) is responsible in both the cases. The difference in lifetimes is probably due to the host material. Further experiments are in progress.



**Figure 7** Emission spectra of fs irradiated PMMA.

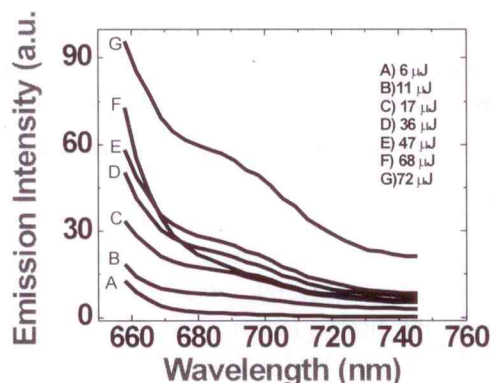


**Figure 8** Emission spectra of fs irradiated PDMS.

Figures 7 and 8 show the emission spectra collected from the fs modified regions of PMMA and PDMS recorded as a function of increasing energies and excited

at 488 and 633 nm, respectively. The emission was collected using a confocal microscope. The fs-modified regions of PMMA exhibited strong emission in the spectral regions of  $\sim 540$  nm. We contemplate the observed emission could be from the defects generated due to bond scission of PMMA [8]. Formation of color centres in our case is ruled out since the absorption/transmission spectra recorded before and after irradiation did not display any additional peaks in the visible region. The possibility of emission from fs-modified PMMA due to free radicals is not considered since the emission was observed even few months after exposure. The cause of emission in PDMS, depicted in figure 7, could be from the defects generated similar to the PMMA case.

## Conclusions

Femtosecond laser irradiated and modified regions of PMMA and PDMS have been characterized using Raman, ESR and Fluorescence. In case of Raman, broadening of modes clearly indicates structural disordering due to pressure. ESR studies lead us to understand free radical formation in the regions of modification and observation of fluorescence is due to interaction of modified region with that of atmospheric oxygen.

## Acknowledgements

Financial support from DST (SR/S2/LOP-11/2005) and funding from CSIR are acknowledged.

## References

1. X. Liu X, D. Du and G. Mourou, J. Quantum Electron. IEEE 33, 1706 (1997).
2. K. Venkatakrishnan, B. Tan and B. K. A. Ngoi, Opt. Eng. 40, 2892 (2001).
3. K. Venkatakrishnan, B. K. A. Ngoi, P. Stanley, B. Tan and L. E. N. Lim, Appl. Phys. A 74, 493 (2002).
4. C. Momma, B.N. Chichkov, S. Nolte, F. Von Alvensleben, A. Tunnermann, H. Welling, B. Wellegehausen, Opt. Commun. 129, 134 (1996).
5. Y. Kondo, K. Nouchi and T. Mitsuyu, Opt. Lett. 24, 646 (1999).
6. R.R. Gattass, and E. Mazur, Nat. Phot. 2, 219-225 (2008).
7. S. Juodkazis, V. Mizeikis, H. Misawa, J. Appl. Phys. 106, 051101 (2009).
8. Z. Nie, H. Lee, H. Yoo, Y. Lee, Y. Kim, K.-S. Lim, M. Lee, Appl. Phys. Lett. 94, 111912 (2009).